J. Condensed Matter Nucl. Sci. 39 (2025) 185–195

Research Article

Encoding Qubits using the Anti-Stokes Peak from a Working CF/LANR Nanomaterial

Dr. Mitchell R. Swartz

JET Energy, Inc.

Abstract

MIT researchers used two slightly different frequency lasers to manipulate nuclear spin. We somewhat copied that with CF/LANR anti-Stokes emission. With additional coherent reflection, these two close-in-frequency photons dramatically impacted the photon polarization of downstream optics. There was significant coherence, with a coherence time of up to an hour. With Qubit encoding, this enables quantum computing. A NAND gate was made.

Keywords: Qubits, Anti-stokes peak, Cold fusion, Lattice assisted nuclear reaction, Coherence, Quantum computing, Photon polarization

1. Introduction and Scope

We previously reported the use of preloaded CF/LANR components, and discovered their anti-Stokes emissions only when they were successful making excess heat [1], [2], [3] (Figure 1). Then, last year, MIT RLE researchers proposed that two slightly different frequency lasers can manipulate nuclear spin [4], [5], [6]. Here, we attempted to copy this with the anti-Stokes emissions from the optical CF/LANR output which specifically involves two close-in-frequency phonon-coupled CF/LANR photon emissions. We have discovered that these two close frequency CF/LANR-induced emissions dramatically impact resultant polarization and output downstream in this optical nanomaterial system (Figure 2). These anti-Stokes emissions, handled correctly, enable quantum computing [7].

These emissions, which encode qubits in this system from a successful working CF/LANR component, are not picked up in the absence of coherent red or green irradiation. However, with either coherent irradiation, there is an increase in emission of photon polarized light in this three polarizer optical system. These results reveal that the anti-Stokes LANR/CF emissions can be used to influence a quantum polarization system (Figures 3 through 6). Furthermore, using these CF/LANR encoded qubits of quantum information (Figure 1), we have made a NAND (not AND) gate, demonstrating that this may enable a new type of quantum computing system with high coherence.

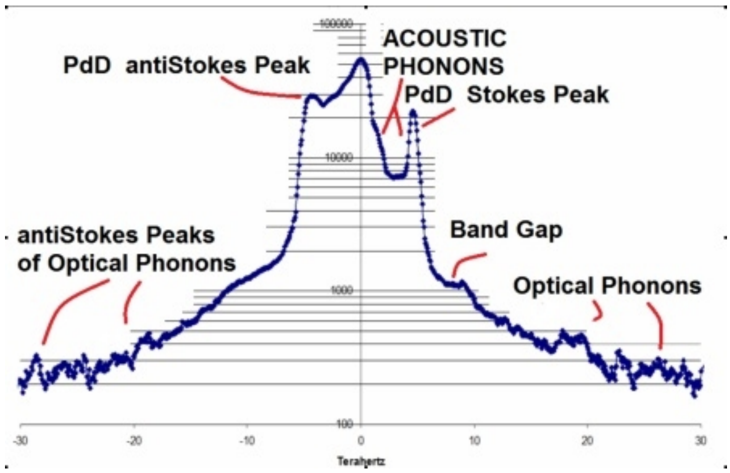

Figure 1. Raman Spectrum obtained during Excess Heat Mode [desired, non-avalanche]. This is a logarithmic presentation of Dual Wavelength Electric-Driven Volume-Enhanced Reflection Spectroscopy of a preloaded, correctly-driven, ZrO_2PdD NANOR®-type Component. The x-axis here presents the frequency difference from the main laser frequency. Identified are the Stokes and anti-Stokes peaks of PdD, and the band gap between acoustic and optical phonons.

2. Background

2.1. Successful LANR Requires Considerable Engineering

LANR success is rewarded by "excess heat", which means that the energy producing reactions have generated *de novo* helium into the lattice ($\sim 10^{12}$ for every watt-second), and there were adequate conditions to enable energy transfer to the lattice and then to appear as excess heat [8]. However, the LANR method which Fleischmann and Pons first taught in March 1989 (aqueous, low impedance, $Pd/D_2O/Pt$) had problems, including inefficiency and non-reproducibility. This created havoc for those inexperienced in metallurgy, electrochemistry, and physics, which generated an intense public glare on this subject.

One major problem to achieve successful cold fusion has been the difficulty in achieving high D/Pd loadings above $\sim$0.70 near room temperature, and then maintaining that sometimes for weeks. In most initial efforts, loading was not even considered even though full loading of the cathodic Pd lattice does promote deuteron fusion. Simply put, really good success requires high loading of >85% for $\mathrm{PdD_x}$ hydrides [8]. This is discussed more in the ICCF24 paper on Deuteron Synchronization [9]. However, full loading of PdD is quite complicated and there are many issues not being considered fully here. First, not all of the available sites are filled, and many of those available sites may not be relevant or even involved.

Second, in addition we now know, by closely looking at the sideband deuterium-line radiofrequency CF/LANR emissions, that at least one of the normally expected vacancy sites slightly change its position during achieving excess heat. In addition, at least one site also changes magnetically and others become pulsatile, all on their RF deuterium-line emissions [10], [11], [12].

Third, most importantly for enabling CF/LANR results, full filling of PdD by loading eliminates the need for deuteron proximity first, and then makes the coulomb barrier moot [9].

Thus, first the previous necessity for deuteron proximity is overcome because the deuterons are Bosons and interact in synchronous reactions. The CF/LANR excess heat production follows, and can be seen in the RF emission

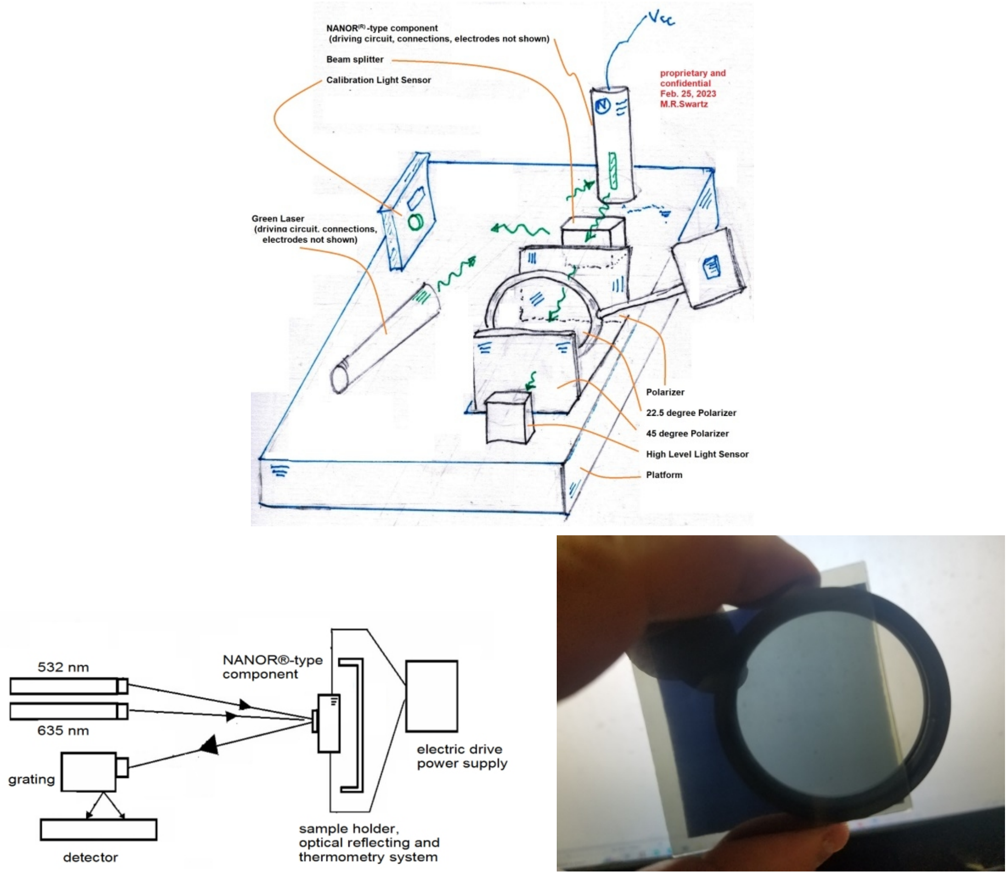

Figure 2. Schematic of CMORE controlled Polarization Qubit System. This is a Qubit Computer, controlled by the CF/LANR component which is shown. The upper figure shows the laser, NANOR®-type component, three linear polarizers and light measurement detectors. The laser is used to reflect off the surface of a NANOR®-type component, yielding the reflected laser beam with the anti-Stokes component ONLY if the NANOR® LANR component is active and working making excess heat. The LANR-associated emitted optical light passes through three linear polaroid filters, into two types of light sensors. On the bottom right, the interposed third polarizer can be seen to increase the optical output which is normally totally blocked by the front and back polarizers.

sidebands, and especially in the pulsating behavior of some of those RF sideband emission lines. Elimination of the need for deuteron proximity, makes moot the normally-expected 'coulomb barrier' which becomes moot thereby in real CF/LANR.

Other problems to achieve successful cold fusion have included the control of vacancies, adequate incubation time, concomitant flux, inadvertent quenching conditions, and lack of critical control of input power. Many "negative" results are due to a failure to operate the system at the optimal operating point, which is observed as an optimum peak in the excess heat and power gain curves as a function of input electrical power.

In summary, the major CF/LANR problems with loading, and later with optimal operating point manifolds and their operation (OOPs) are why initial efforts to replicate successful LANR were so difficult and failed to show excess heat.

2.2. Dry Preloaded NANOR®-type CF/LANR Components

Dry preloaded NANOR®-type LANR (lattice assisted nuclear reaction) components have been described in the literature [13]–[16]. A NANOR®-type component is a hermetically sealed CF/LANR [cold fusion/lattice assisted nuclear reactions] nanomaterial component, preloaded with D and arranged as a two-terminal electrical component. They are the size of an ohmic resistor, and are designed to avoid leakage, enabling stabilization and activation of these materials. The central core generating the excess heat in the desired state contains ZrO_2PdNiD, ZrO_2PdD, and ZrO_2NiD and similar materials. NANOR ®-type components have been used to investigate material science and radiation physics of their active LANR systems. These reports were expanded to demonstrate that several electrical transconduction states exist, but that only one is active, desired, and capable of producing "excess heat" [17], [18].

2.3. Anti-Stokes Peaks of Successful PdD LANR

We have previously demonstrated that when NANOR®-type components are electrically driven to produce excess heat, there is a large antiStokes component [1], [2], [3]. Simply put, without anti-Stokes emissions, there is no evidence of real CF/LANR excess heat. By contrast, successful cold fusion is saliently heralded by a large increase in the anti-Stokes to Stokes (aS/S) ratio. This XSH-related peak is singular and at slightly higher energy. Our two-terminal preloaded deuterided NANOR®-type CF/LANR components have a measured Boltzmann Stokes ratio $\sim$1.3, only when active with XSH.

Previously our findings have been used to confirm a role for PdD acoustic phonons in successful CF/LANR. This was done because Raman spectroscopy is a powerful tool to study vibrations within molecules, materials, and nanostructured materials to obtain knowledge of the momentum, intensity, internal temperature and energies from the returned optical spectrum. The lack of coherence by laser is why Raman originally had such a hard time. At his Nobel lecture he complained the Raman spectra were very low level outputs, but here with the coherent input, the output intensity of these are 10^6 times greater.

By important contrast, we have demonstrated that CMORE coherent spectroscopy [1], [2], [3], based on Raman spectroscopy, would be quite useful in distinguishing active LANR states because they are electrically driving them at their peak optimal operating point (Figure 2).

This report expands that and shows (confer Figure 1) that for successful LANR, the anti-Stokes component matches the Stokes component for PdD. By contrast, non-active, unsuccessful, electrical avalanches have never produced excess heat, and have anti-Stokes components that match the ZrO_2 Stokes components and not those of PdD.

2.4. What is a Qubit

A qubit is a two-level quantum-mechanical system [7]. Examples include electron spin ["up" and "down"] and photon polarization [vertical and horizontal polarization]. However, the strangest, most unusual, properties of qubits is that they exhibit superposition and as a result, the qubit can also be a coherent superposition of both states at the same time, a mixed combination of 1 and 0. Superposition appears when they interact with something else. Here, photon polarization will interact with the antiStokes emission of a working CF/LANR NANOR®-type component. There are several issues and implications to now consider about qubits. First, a qubit can hold more information [up to two bits using superdense coding]; and for *n* components, in classical physics there are *n* bits in total. However, quantum physics yields 2^n complex numbers.

2.5. Quantum Entanglement – Fragile Coherence and Decoherence

Even more importantly, unlike conventional classical bits, multiple qubits exhibit quantum entanglement. This is a "nonlocal" property where two sets of qubits express a higher correlation than is possible in any classical system. In other words, entanglement enables multiple qubits – at separate locations (which can be distant) – to astonishingly share a common quantum state.

This occurs no matter how far apart the qubit sets are, and enables quantum teleportation, entangled quantum cryptography and superdense coding. However, quantum entanglement is fragile. On the down side, even quantum measurement becomes an irreversible operation because as information is gained/revealed about the state of a single qubit, its coherence is lost. Thereafter, as qubit entanglement and superposition collapse, the quantum qubit "decoheres." Decoherence can occur several ways, including oxidation, and decoherence limits qubit efforts today.

2.6. Historical Platforms of Qubits

The platform for making/using qubits are ions, photons, and other select semiconductors and materials. Some are useful for quantum computing, others for quantum sensing or quantum communication. The first qubit was made from a single beryllium ion. Another qubit device uses diamonds where some of the carbon atoms are replaced by nitrogen atom or vacancies. The trapped ions in the lattice vacancies store information as spin. The largest trapped-ion quantum computer is the 32-qubit information device made by IonQ, College Park, Maryland. The superconducting qubit is a trapped-ion qubit, cooled to a few hundredths of a degree above absolute zero, held by an oscillator circuit. Radio photons have been shown to move the circuit to the second energy level or a superposition of the two states. IBM made a 1,121-qubit device by 2023.

2.7. Current Problems of Qubits

Today, the existence of quantum computers is limited by the lack of a reliable method to encode qubits. This month, MIT RLE researchers have proposed using two slightly different frequency lasers, to manipulate nuclear spin [4], [5], [6]. Previously, this was attempted using indirect coupling which is susceptible to noise. However, the MIT method reportedly improves coherence times, now to hours, and is called the optonuclear quadrupolar [ONQ] effect. This ONQ effect is second order on the electric field and nuclear spin, and is mediated by the quadrupole electric coupling, making it a nonlinear optical (NLO) response of a lattice.

3. Experimental Qubits

3.1. Methods

The plan is to use the optical output from a CF/LANR working component. What is most interesting is how the optical output from these working CF/LANR heat producing components can be used to generate entangled quantum computers. Our goal is to use the two slightly different frequency laser effect discovered at MIT to coherently control polarization, by the two near-frequency photons. Here the reflected photons and phonon-derived anti-Stoke photons are used to more efficiently control photon polarization and thus encode qubits. This effect may teach further understanding of the CF/LANR processes and their possible interaction(s) with quantum devices.

Figure 2 shows a Qubit Computer controlled by the CF/LANR component. which is set up and used as shown below. This is a CMORE controlled Polarization Qubit System. CMORE is Coherent optical reflection electric-driven spectroscopy. Figure 2 shows a laser which is used to reflect off the surface of a NANOR being in the "off", XSH-producing, or electrical avalanche state. After a beam splitter, (or directly) the reflected laser beam and the antiStokes component, if the NANOR is working, pass through three linear polaroid filters, into two types of light sensors. The components were mounted in a 3D printed set of black PLA wells and tunnels (not shown).

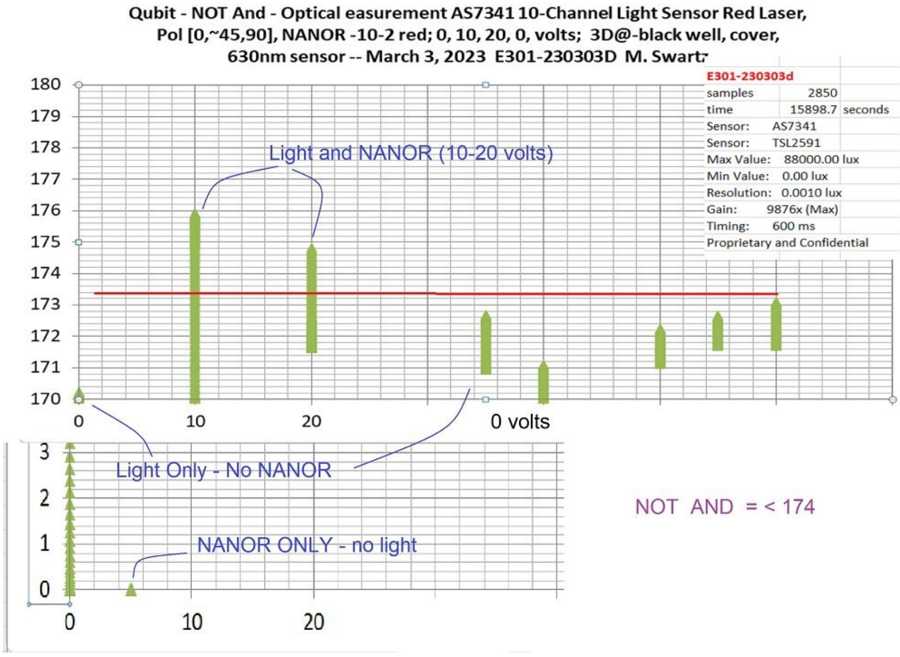

Figure 3. Qubit system showing slight increase in light at 630 nM driven by the CF/LANR antiStokes emissions of NANOR®-type component 10-2-red. The horizontal axis is the voltage applied across the NANOR®-type component, with a peak of twenty volts, and then it returned to zero (although the laser continues without change).

3.2. Light Measurement

The AS7341 10-Channel Light/Color Sensor was used as one of the light sensors. It is a multi-channel spectrometer in a 3x2mm opening with 16 different types of sensors that detect eight separate, overlapping bands of colored light, white light, and Near Infra-red light. The output of the sensors is routed through a 16-bit 6-channel ADC using multiplexing with a Super MUX (SMUX). The second sensor is an ultra-high-range luminosity sensor using the TSL2591 advanced digital light sensor. This enables detection of 188 microLux up to 88,000 Lux. This sensor is much like the TSL2561 but with a wider range (and the interface code is different). This sensor has a massive 600,000,000:1 dynamic range. The Lux is calculated. The infrared and visible spectrum sensor data is correlated with the equivalent SI lux value. The value is improved based upon a table using the specific sensor properties, the integration time and the gain settings. This data, along with the infrared and visible spectrum sensor data as raw 16-bit values, were used.

4. Results

4.1. Qubit Encoding with NANOR type components

In summary, the normally-invisible antiStokes emissions from either NANOR electrically-driven have worked enabling Qubit encoded results. These are seen as influencing the optical linear polarization throughput beyond the 3 polarizers in the optical path. This Qubit influence occurred for both 0, ∼22.5 and 45 degrees, and 0, ∼45, and 90 degrees, setups of the polarizing filters. Both of the arrangements of the polarizers worked with an astonishing Qubit encoding. This can be seen in the graphs which show several runs; with a range optical Qubit encoded outputs for each of several applied voltages (including zero volts).

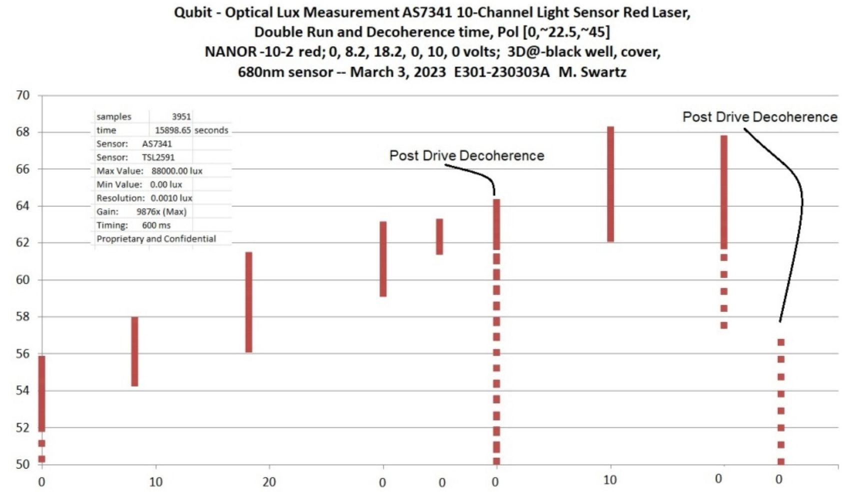

Figure 4. Qubit Encoding System showing slight increase at 680 nM using CF/LANR antiStokes at 8.2, 18.2, and 10 volts across NANOR®-type component 10-2-red. In this double run, increasing sensitivity is noted, along with a long decoherence time. The horizontal axis is the voltage applied across the NANOR®-type component, with a peak of twenty volts, and then it returned to zero (although the laser continues without change).

4.2. The NANOR Type Components Alone Had Indetectable Optical Output

The NANORs gave NO optical output which could be detected in the absence of laser irradiation. Specifically, when electrically driven, the NANOR components gave off no light which could be picked up by the sensors even with maximum sensitivity, only in the absence of the red or green laser also on it.

4.3. The Irradiated NANOR Type Components Had Detectable Optical Output

However when either of the lasers were on to provide coherent irradiation of the driven NANOR-type component, the result increased the throughput polarization by a small amount. With the laser irradiation in either the red or green enabled, there were small, often voltage-related increases in the polarized light put through the three polarizing filters. The irradiated coherent light on the electrically-driven NANOR type components did give changes in the polarization output detected; they increased the polarization throughput by a small amount (Figures 3 to 6).

In the Figures, these Qubit encoded outputs are shown as they were seen post-polarizer, as outputs at both 680 nM and 630 nM over time, with increasing NANOR electrical drive. There were usually slight increases at both 630 nM and 680 nM with antiStokes. The LUX output was less useful and was more complicated because of its continuous drift, and initial peaks. Sometimes an initial peak was seen in the lux calculations. We believe that the first peak resulted from the initial IR changes, which continued until the secondary temperature no longer increased as the heat flows, and with the heat flow a steady state is achieved. For this reason, and the drift, the focus was mainly on the two 630 and 680 nanometer values.

4.4. Problems

The biggest problem initially was using green lasers to get the antiStokes, consistent with the original papers. This did not work very well because each sensor contains at least one green LED showing electrical activity involving that

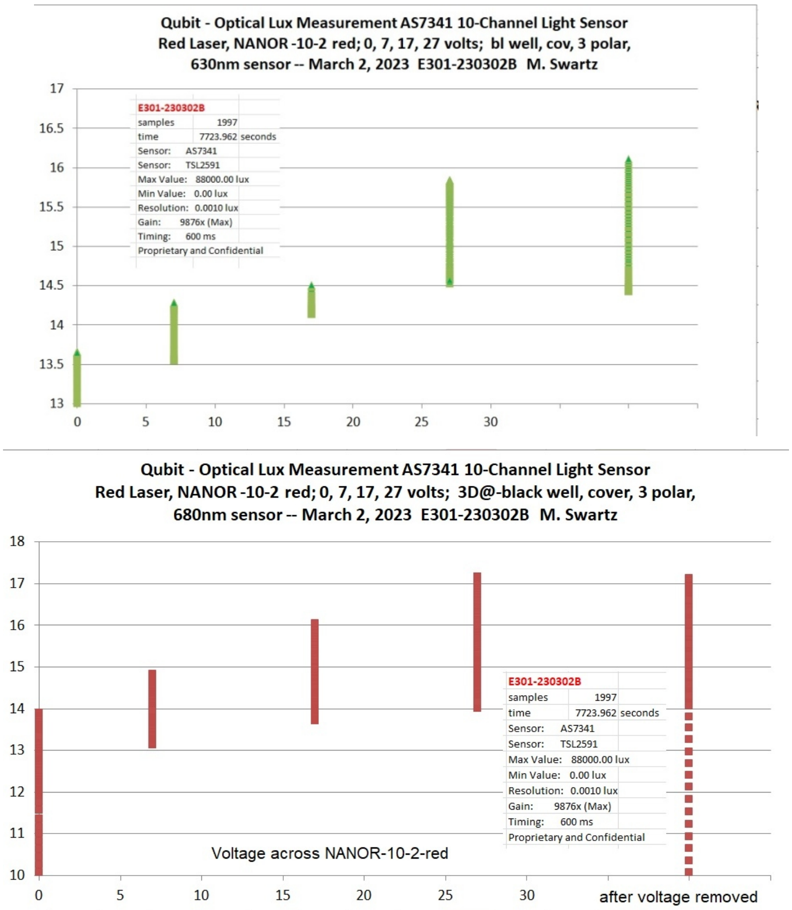

Figure 5. Qubit Encoding System showing slight increases in light at 630 nM (top) and 680 nM (bottom) driven by the CF/LANR antiStokes emissions. The horizontal axis is the voltage applied across the NANOR®-type component, N10-2, with 7, 17, and a peak of twenty seven volts, and then it returned to zero (although the laser continues without change).

chip. Unable to turn them all off, and because small changes were noted, the irradiating light to elicit antiStokes was changed to irradiating coherent light from a red laser instead. In addition, the Nanor®-type component 10-2red had electrical avalanches above circa 30V, so it was important to keep the applied voltage below that.

4.5. Quantum Entanglement – Fragile Coherence and Decoherence

There was significant coherence Demonstration in Figures 3, 4, 5 and 6 show that entanglement from NANOR components in these Qubit Encoding systems can have long coherence time. On those occasions, although the observed increase seen mostly disappeared when the voltage across the driven CF/LANR component went to zero, there was an increase slightly before falling of the output. Those runs showed a coherence time of almost an hour (usually less).

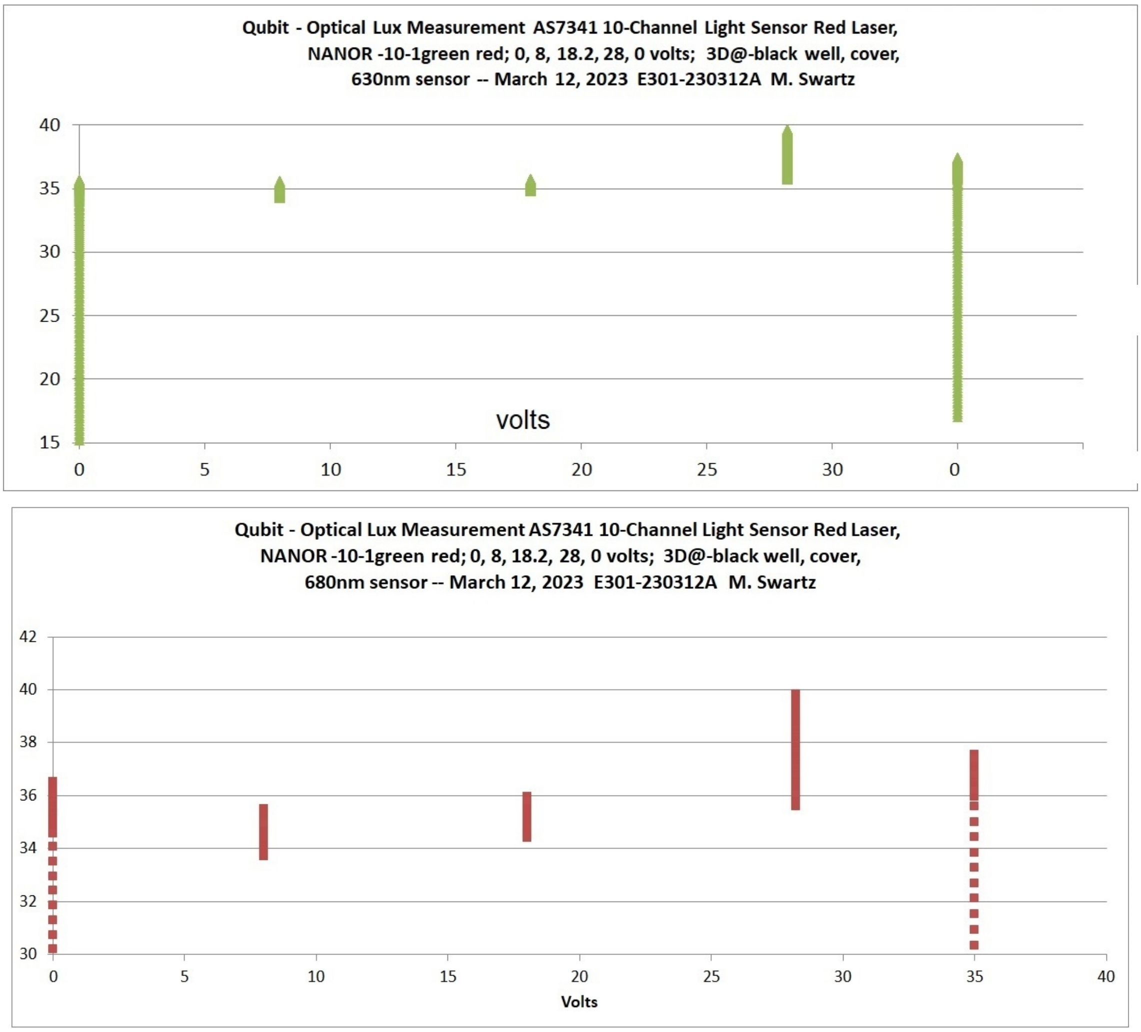

Figure 6. Qubit Encoding System showing slight increases in light at 630 nM (top) and 680 nM (bottom) driven by the CF/LANR antiStokes emissions. The horizontal axis is the voltage applied across the second NANOR®-type component, N10-1, with 8, 18.2, and a peak of 28 volts, and then it returned to zero (although the laser continued without change).

Figure 4 shows that sometimes an increased sensitivity occurs, such as that shown in the second run which had a larger output.

4.6. Encoded Qubits May Enable New Quantum Computing Systems

Using these CF/LANR encoded qubits, we have made a NAND gate, demonstrating that this may enable a quantum computing system with high coherence. That complicated coherent computation systems results because by combining NAND, NOR and NOT gates, one can also configure AND, OR, XNOR and XOR gates, too.

5. Conclusion

5.1. Encoded Qubits Using antiStokes Emissions from CF/LANR Components

In summary, anti-Stokes emissions from successfully electrically driven preloaded CF/LANR components can couple in quantum systems to dramatically impact resultant polarization and output downstream in Qubit systems which enables encoding with high coherence. The two close frequency anti-Stokes emissions are picked up by coherent red or green irradiation. Because these anti-Stokes LANR/CF emissions can be used to influence a quantum polarization system, they may enable new types of quantum computing systems.

These novel quantum coupled computing systems may open up new possibilities for CF/LANR components far beyond simply making the long desired excess heat available from their highly loaded condensed materials.

Acknowledgments

The author gratefully acknowledges and thanks, for their helpful comments, editorial assistance, and suggestions: Joshua Gyllinsky, Gayle Verner, Isidor Straus, John Wallace, and Peter Hagelstein. This effort was supported by JET Energy Inc. NANOR® is a registered trademark.

References

[1] Swartz, M.R., Hagelstein, P.L., Increased PdD anti-Stokes Peaks are Correlated with Excess Heat Mode, J. Condensed Matter Nucl. Sci. 24, 130–145 (2017).

[2] Swartz, M. R, Increase of an Anti-Stokes Peak at the Cathode of an Electrically-Driven, Active Aqueous Nickel/H_2O/Pt System, J. Cond Matter Nucl. Sci., Vol 27, 22–29 (2018).

[3] Swartz, M.R. "Optical Detection of Phonon Gain Distinguishes an Active Cold Fusion/LANR Component", JCMNS, 20, 29–53 (2016).

[4] Haowei Xu, Changhao Li, Guoqing Wang, Hua Wang, Hao Tang, Ariel Rebekah Barr, Paola Cappellaro, and Ju Li, Two-Photon Interface of Nuclear Spins Based on the Optonuclear Quadrupolar Effect, Phys. Rev. X 13, 011017, February 14, 2023; https://journals.aps.org/prx/abstract/10.1103/PhysRevX.13.011017

[5] David L. Chandler, MIT Spins Qubits Round And Round, MIT News, February 15, 2023. https://news.mit.edu/2023/engineers-discover-new-way-control-atomic-nuclei-qubits-0215

[6] Al Williams, MIT Spins Qubits Round And Round, February 16, 2023. https://hackaday.com/2023/02/16/mit-spins-qubits-round-and-round/

[7] Benjamin Schumacher, (1995). "Quantum coding". Physical Review A **51** (4): 2738–2747. Bibcode:1995PhRvA..51.2738S. doi:10.1103/PhysRevA.51.2738. PMID, 9911903

[8] Swartz, M., "Survey of the Observed Excess Energy and Emissions In Lattice Assisted Nuclear Reactions", Journal of Scientific Exploration, 23, 4, 419–436 (2009).

[9] Swartz, M. R., Synchronization of Vacancy-Loaded Deuterons Enables Successful LANR Mass-Energy Transfer, JCMNS, Proceedings of ICCF24, Vol. 38, 147 (May 2024).

[10] Swartz, M. R, FCC Vacancies in ZrO2PdD RF are the Active LANR Site, Proc. ICCF-22, J. Cond.Matter Nucl. Sci., Volume 33, pages 126–144 (2020).

[11] Swartz, M. R, Active LANR Systems Emit a 327.37 MHz Maser Line, Proc. ICCF-22, J. Condensed Matter Nucl. Sci., Volume 33, pages 80–110 (2020).

[12] Swartz, M. R, Pulsatile Superhyperfine Lines at 327.37 MHz Herald LANR Activity and Possible Mass-Energy Transfer, Proc. ICCF-22, J. Condensed Matter Nucl. Sci. , Volume 33, pages 111-125 (2020).

[13] Swartz M. R., Verner G., Tolleson, J, Energy Gain From Preloaded ZrO_2–PdNi–D Nanostructured CF/LANR Quantum Electronic Components, J. Condensed Matter Nucl. Sci. 13, 528, (2014).

[14] Swartz M. R., Hagelstein P.I., Demonstration of Energy Gain from a Preloaded ZrO_2–PdD Nanostructured CF/LANR Quantum Electronic Device at MIT, *J. Condensed Matter Nucl. Sci.* 13, 516, (2014).

[15] Swartz M. R., Incremental High Energy Emission from a ZrO2–PdD Nanostructured Quantum Electronic Component CF/LANR, J. Condensed Matter Nucl. Sci. 15, 92 (2015).

[16] Swartz M.R., Verner, G., et al., Imaging of an Active NANOR®-type LANR Component using CR-39, J. Condensed Matter Nucl. Sci. 15, p 81 (2015).

[17] Swartz, M.R. P. Hagelstein, G. Verner, Impact of Electrical Avalanche Through a ZrO2-NiD Nanostructured CF/LANR Component on its Incremental Excess Power Gain", ICCF-19, JCMNS, 19, (2016).

[18] Swartz, M. R, Aqueous and Nanostructured CF/LANR Systems Each have Two Electrically Driven Modes, Proc. ICCF-21, Fort Collins, Co.6/3/18 (2018), J. Condensed Matter Nucl. Sci, Vol 29, 177 (2019).